

# Effect of Cholesterol on Molecular Order and Dynamics in Highly Polyunsaturated Phospholipid Bilayers

Drake C. Mitchell and Burton J. Litman

Section of Fluorescence Studies, Laboratory of Membrane Biophysics and Biochemistry, National Institute on Alcohol Abuse and Alcoholism, National Institutes of Health, Rockville, Maryland 20852 USA

**ABSTRACT** The effect of cholesterol on phospholipid acyl chain packing in bilayers consisting of highly unsaturated acyl chains in the liquid crystalline phase was examined for a series of symmetrically and asymmetrically substituted phosphatidylcholines (PCs). The time-resolved fluorescence emission and decay of fluorescence anisotropy of 1,6-diphenyl-1,3,5-hexatriene (DPH) was used to characterize equilibrium and dynamic structural properties of bilayers containing 30 mol % cholesterol. The bilayers were composed of symmetrically substituted PCs with acyl chains of 14:0, 18:1n9, 20:4n6, or 22:6n3, containing 0, 1, 4, or 6 double bonds, respectively, and mixed-chain PCs with a saturated 16:0 *sn*-1 chain and 1, 4, or 6 double bonds in the *sn*-2 chain. DPH excited-state lifetime was fit to a Lorentzian lifetime distribution, the center of which was increased 1–2 ns by 30 mol % cholesterol relative to the cholesterol-free bilayers. Lifetime distributions were dramatically narrowed by the addition of cholesterol in all bilayers except the two consisting of dipolyunsaturated PCs. DPH anisotropy decay was interpreted in terms of the Brownian rotational diffusion model. The effect of cholesterol on both the perpendicular diffusion coefficient  $D_{\perp}$  and the orientational distribution function  $f(\theta)$  varied with acyl chain unsaturation. In all bilayers, except the two dipolyunsaturated PCs, 30 mol % cholesterol dramatically slowed DPH rotational motion and restricted DPH orientational freedom. The effect of cholesterol was especially diminished in di-22:6n3 PC, suggesting that this phospholipid may be particularly effective at promoting lateral domains, which are cholesterol-rich and unsaturation-rich, respectively. The results are discussed in terms of a model for lipid packing in membranes containing cholesterol and PCs with highly unsaturated acyl chains.

## INTRODUCTION

In recent years, evidence has accumulated supporting the hypothesis that biological membranes are organized in distinct lateral domains or microdomains (for review, see Bergelson et al., 1995). The types of domains that have been characterized or inferred vary from the macroscopic domains isolated in the plasma membranes of a variety of epithelial cells to microdomains consisting of a small number of lipid molecules (reviewed in Schroeder and Wood, 1995). One of the most frequently discussed types of microdomains are those characterized as cholesterol rich and cholesterol poor. A number of studies have detected cholesterol-dependent lateral domains in model bilayer systems. Immiscible cholesterol-rich and cholesterol-poor fluid phases have been observed by deuterium NMR in bilayers consisting of saturated phosphatidylcholines with cholesterol (Sankaram and Thompson, 1990; Vist and Davis,

1990). Several investigations of cholesterol in bilayers consisting of unsaturated phospholipids have concluded that acyl chain unsaturation plays a role in creating separate cholesterol-rich and unsaturation-rich microdomains. A number of electron spin resonance investigations of cholesterol in 16:0, 18:1 PC and di-18:1 PC bilayers have demonstrated fluid-phase microimmiscibility leading to cholesterol-rich and cholesterol-poor domains, and the lifetime of such microdomains is estimated to be 1–100 ns (Pasenkiewicz-Gierula et al., 1990, 1991; Subczynski et al., 1990). A series of monolayer, differential scanning calorimetry, and fluorescence studies involving high levels of acyl chain polyunsaturation and cholesterol have been interpreted as providing evidence for coexisting cholesterol-rich and unsaturation-rich microdomains (Stillwell et al., 1994, 1996; Zerouga et al., 1995).

Many important biological membranes, such as those found in the nervous system, retina, and spermatozoa, contain an appreciable amount of phospholipid with two polyunsaturated acyl chains as well as mixed-chain phospholipids with one polyunsaturated acyl chain (Salem, 1989). A primary goal of our current study was to differentiate the effects of cholesterol on mixed-chain *sn*-1 saturated, *sn*-2 unsaturated phospholipids from those of cholesterol on symmetrically unsaturated phospholipids. Recent interest in this area has focused on the effects of cholesterol on bilayers containing highly polyunsaturated acyl chains (four or more double bonds). Monolayers of phospholipids with one or both acyl chains derived from docosahexaenoic acid (22:6n3) are not condensed by 50 mol % cholesterol (Zer-

Received for publication 28 January 1998 and in final form 4 May 1998.

Address reprint requests to Dr. Drake C. Mitchell, NIAAA, Park Building, Room 158, 12420 Parklawn Drive, Rockville, MD 20852. Tel.: 301-443-1102; Fax: 301-594-3608; E-mail: dmitchell@niaaa.nih.gov.

Abbreviations used in this paper: 16:0, 18:1 PC, 1-palmitoyl-2-oleoyl-*sn*-glycero-3-phosphocholine; 16:0, 20:4 PC, 1-palmitoyl-2-arachidonoyl-*sn*-glycero-3-phosphocholine; 16:0, 22:6 PC, 1-palmitoyl-2-docosahexaenoyl-*sn*-glycero-3-phosphocholine; di-14:0 PC, 1,2-dimyrtoyl-*sn*-glycero-3-phosphocholine; di-18:1 PC, 1,2-dioleoyl-*sn*-glycero-3-phosphocholine; di-20:4 PC, 1,2-diarachidonoyl-*sn*-glycero-3-phosphocholine; di-22:6 PC, 1,2-didocosahexaenoyl-*sn*-glycero-3-phosphocholine; BHT, butylated hydroxytoluene; DPH, 1,6-diphenyl-1,3,5-hexatriene; LC, liquid crystalline; PC, phosphatidylcholine; BRD, Brownian rotational diffusion.

© 1998 by the Biophysical Society

0006-3495/98/08/896/13 \$2.00

ouga et al., 1995). In addition, cholesterol was found to have no effect on the enthalpy of the gel-to-liquid-crystalline phase transition of di-22:6n3 PC (Kariel et al., 1991). Both of these results strongly imply a weak interaction between 22:6n3 phospholipid acyl chains and cholesterol and raise two questions regarding the effect of acyl chain unsaturation on cholesterol-acyl chain interactions. The first question is whether or not the weak interaction with cholesterol is specific to highly unsaturated n3 species or might also apply to highly unsaturated n6 phospholipid acyl chains. The second question is the relative importance of high levels of unsaturation on one acyl chain versus symmetric unsaturation of both phospholipid acyl chains with regard to weakening the interaction with cholesterol.

To answer these questions we have measured the effects of 30 mol % cholesterol on DPH excited-state lifetimes and anisotropy decays in LC phase bilayers consisting of PCs with 18:1n9, 20:4n6, or 22:6n3 occupying both acyl chain positions or occupying only the *sn*-2 position with a 16:0 acyl chain at the *sn*-1 position. DPH is an ideal probe of the hydrophobic bilayer core for this type of investigation because it partitions equally between di-16:0 PC and di-22:6 PC vesicle populations when both are in the liquid crystalline phase (Niebylski and Litman, unpublished). We also examined cholesterol in di-14:0 PC to compare the effect of cholesterol on acyl chain order in an unsaturated phospholipid with a disaturated phospholipid. The angular probability distribution of DPH in these cholesterol-containing bilayers was obtained via analysis of anisotropy decay data in terms of the BRD model. The probability distribution is interpreted as reflecting acyl chain ensemble order throughout the depth of the bilayer (Mitchell and Litman, 1998). Comparison of the cholesterol-induced changes in the DPH angular distribution function revealed the detailed manner in which acyl chain composition modulates cholesterol's ability to increase acyl chain ensemble order at different depths in the bilayer.

## EXPERIMENTAL PROCEDURES

All phospholipids, di-22:6n3 PC, di-20:4n6 PC, di-18:1n9 PC, di-14:0 PC, 16:0, 22:6n3, 16:0, 20:4n6, and 16:0, 18:1n9 PC, were purchased from Avanti Polar Lipids (Alabaster, AL) and, after purity was checked with high performance liquid chromatography, used without further purification. All polyunsaturated species were packaged by Avanti with BHT at a BHT:phospholipid ratio of 1:300. Cholesterol was purchased from Calbiochem (La Jolla, CA), and DPH was purchased from Molecular Probes (Eugene, OR). Cholesterol was dissolved in chloroform that contained 75  $\mu$ M BHT and added to the required amount of phospholipid in chloroform to give a molar ratio of cholesterol:phospholipid of 3:7. Large unilamellar vesicles were made as previously described (Mitchell and Litman, 1998) and extruded 10 times through a pair of 0.2- $\mu$ m membranes using a Lipex extruder (Vancouver, British Columbia, Can-

ada). After vesicle preparation, the final phospholipid concentration was determined (Bartlett, 1959), and final cholesterol concentration was measured with a standard cholesterol assay kit using cholesterol oxidase (Sigma Chemical Co., St. Louis, MO). All procedures involving unsaturated phospholipids were carried out in an airtight glove box, constantly flushed with argon.

## Fluorescence measurements

Fluorescence lifetime and differential polarization measurements were performed with a K2 multifrequency cross-correlation phase fluorometer (ISS, Urbana, IL). Excitation at 351 nm was provided by an Innova 307 argon ion laser (Coherent, Santa Clara, CA). Lifetime and differential polarization data were acquired using decay acquisition software from ISS at 10, 20, 30, and 40°C, except for di-14:0 PC, which was studied at 30, 40, 47, and 55°C. For lifetime measurements, 12 modulation frequencies were used, logarithmically spaced from 5 to 250 MHz. All lifetime measurements were made with the emission polarizer at the magic angle of 54.7° relative to the vertically polarized excitation beam and with 1,4-bis(5-phenyloxazol-2-yl)benzene in absolute ethanol in the reference cuvette ( $\tau = 1.35$  ns; Lakowicz et al., 1981). Differential polarization measurements were made at 15 modulation frequencies logarithmically spaced from 5 to 300 MHz. For each differential polarization measurement, the instrumental polarization factors were measured and found to be between 1 and 1.05, and the appropriate correction factor was applied. Scattered excitation light was removed from the emission beam by a 390-nm highpass filter. At each frequency, data were accumulated until the standard deviations of the phase and modulation ratio were below 0.2 and 0.004, respectively, and these values were used as the standard deviation for the measured phase and modulation ratio in all subsequent analysis. Both total intensity decay and differential polarization measurements were repeated at each temperature with each bilayer composition a minimum of three times.

## Data analysis

Total fluorescence intensity decays were modeled with a Lorentzian distribution plus a discrete exponential decay to account for scattered background light, using Globals Unlimited (Alcala et al., 1987; Beechem et al., 1991). The lifetime of the discrete component was fixed at 0.001 ns, and its fractional intensity was allowed to vary along with the center of the Lorentzian distribution  $\tau_c$  and the width of the distribution at half-height  $w$ . The resulting fractional intensity of the discrete component varied from 0.5% to less than 0.1%, and the values of reduced  $\chi^2$  ranged from 1 to 4.

Measured polarization-dependent differential phases and modulation ratios for each sample were combined with the measured total intensity decay to yield the anisotropy decay  $r(t)$ . All anisotropy decay data were analyzed using the

Brownian rotational diffusion model (BRD model; see Levine and van Ginkel, 1994, for a review), which yields the order parameters  $\langle P_2 \rangle$  and  $\langle P_4 \rangle$  (Szabo, 1984; van der Meer et al., 1984). These two order parameters can be used to construct an orientational distribution function,  $f(\theta)$ , of the probe molecule. All analysis was performed by globally analyzing all of the data at four temperatures for each bilayer composition with  $r_0$  globally linked. This global analysis approach has been demonstrated to reduce the uncertainty in all recovered parameters (Wang et al., 1991; Mitchell and Litman, 1998).

In general, the orientation of a molecule with cylindrical symmetry in a lipid bilayer is completely described by the angle  $\theta$  between its symmetry axis and the local membrane normal. The results of the BRD model-based analysis were interpreted in terms of an angular distribution function that is symmetric about  $\theta = \pi/2$  and is based on maximizing the information entropy of  $f(\theta)$  (van der Meer et al., 1982; Pottel et al., 1986):

$$f(\theta) = N^{-1} \exp[\lambda_2 P_2(\cos \theta) + \lambda_4 P_4(\cos \theta)], \quad (1)$$

where  $\lambda_2$  and  $\lambda_4$  are constants determined by simultaneous solution of equations for  $\langle P_2 \rangle$  and  $\langle P_4 \rangle$  and  $N$  is the normalization constant determined according to

$$N = \int_0^\pi \sin(\theta) \exp[\lambda_2 P_2(\cos \theta) + \lambda_4 P_4(\cos \theta)] d\theta. \quad (2)$$

Analysis of DPH anisotropy decays with the distribution function defined in Eq. 1 results in bimodal orientational distribution functions (van Langen et al., 1987, 1989; van Ginkel et al., 1989; Wang et al., 1991; Mitchell and Litman, 1998) with one population distributed about the bilayer normal and a second, orthogonal population at the bilayer midplane distributed about a plane parallel to the bilayer surface. To assess the relative size of these two populations,

the fraction perpendicular  $f_\perp$  was calculated according to

$$f_\perp = \int_{\pi/4}^{3\pi/4} f(\theta) \sin(\theta) d\theta. \quad (3)$$

The extent to which the equilibrium orientational freedom of DPH is restricted by the phospholipid acyl chains was quantified using the parameter  $f_v$  (Straume and Litman, 1987a), which is defined by

$$f_v = \frac{1}{2 \times f(\theta)_{\max}}. \quad (4)$$

All analyses of differential polarization data were performed with NONLIN (Dr. Michael Johnson, Pharmacology Department, University of Virginia Health Sciences Center, Charlottesville, VA), which uses a modified Gauss-Newton nonlinear least-squares algorithm (Straume et al., 1991; Johnson and Faunt, 1992) with subroutines specifying the fitting function written by the authors. NONLIN accounts for all higher-order correlations that may exist between fitting parameters when determining confidence intervals. The NONLIN software package allows the user to include a subroutine that calculates most probable values and asymmetric confidence intervals of quantities that are calculated from the designated fitting parameters. Use of this subroutine insures accurate propagation of confidence intervals when calculating derived parameters from fitting parameters, for example, when calculating  $f_v$ . Asymmetric confidence intervals equivalent to 1 SD were obtained for both fitting variables and derived parameters.

## RESULTS AND DISCUSSION

### Fluorescence lifetimes

The fluorescence lifetime of DPH, as summarized by the center of the fitted Lorentzian lifetime distribution  $\tau_c$ , varied

**TABLE 1** Centers ( $\tau_c$ ) and widths ( $w$ ) of Lorentzian distributions of DPH fluorescence lifetimes in bilayers containing 30 mol % cholesterol

Phospholipid		10°C	20°C	30°C	40°C
di-22:6 PC	$\tau_c$	8.30 ± 0.08	7.98 ± 0.11	7.68 ± 0.09	7.28 ± 0.12
	$w$	1.07 ± 0.16	0.81 ± 0.21	0.87 ± 0.16	0.78 ± 0.14
di-20:4 PC	$\tau_c$	9.00 ± 0.08	8.81 ± 0.08	8.49 ± 0.06	8.43 ± 0.11
	$w$	1.42 ± 0.16	2.27 ± 0.15	1.31 ± 0.30	1.38 ± 0.21
di-18:1 PC	$\tau_c$	8.91 ± 0.05	8.87 ± 0.10	8.63 ± 0.05	8.23 ± 0.12
	$w$	0.05 ± 0.02	0.05 ± 0.02	0.05 ± 0.2	0.23 ± 0.10
16:0, 22:6 PC	$\tau_c$	9.80 ± 0.11	9.78 ± 0.08	9.31 ± 0.16	9.14 ± 0.07
	$w$	0.05 ± 0.02	0.05 ± 0.02	0.05 ± 0.02	0.71 ± 0.10
16:0, 20:4 PC	$\tau_c$	8.69 ± 0.08	8.63 ± 0.10	8.54 ± 0.12	7.93 ± 0.08
	$w$	0.12 ± 0.07	0.32 ± 0.08	0.36 ± 0.10	0.82 ± 0.18
16:0, 18:1 PC	$\tau_c$	10.53 ± 0.08	10.26 ± 0.20	9.97 ± 0.23	9.89 ± 0.14
	$w$	0.13 ± 0.08	0.05 ± 0.03	0.06 ± 0.01	0.30 ± 0.12
di-14:0 PC	$\tau_c$	ND	ND	10.18 ± 0.06	10.14 ± 0.10
	$w$			0.05 ± 0.02	0.05 ± 0.02

ND, not done.

with both temperature and phospholipid composition in the cholesterol-containing bilayers, as shown in Table 1. An increase in temperature from 10 to 40°C caused a reduction in  $\tau_c$  that ranged from 0.6 to 1 ns in all bilayers. However, the value of  $\tau_c$  at any temperature was strongly dependent upon the phospholipid acyl chain composition. This acyl chain dependence is most apparent when comparing the values of  $\tau_c$  for di-14:0 PC with those in the two dipolyunsaturated PCs. A large variation in  $\tau_c$  was also observed in cholesterol-free bilayers composed of the phospholipids listed in Table 1 (Mitchell and Litman, 1998). A comparison of the effect of cholesterol on  $\tau_c$  is given in Fig. 1 A, demonstrating that at 30°C, 30 mol % cholesterol increases  $\tau_c$  by 1–1.5 ns, or ~15%, in all seven bilayer compositions. Similar differences between  $\tau_c$  values in the presence and absence of cholesterol were found in all phospholipid bilayers examined, which shows that the cholesterol-induced increase in DPH fluorescence lifetime is not acyl chain dependent.

The wide variation in  $\tau_c$  shown in Table 1 is most likely due to changes in water penetration into the bilayer induced

by changes in temperature and acyl chain composition. The decrease in  $\tau_c$  with increasing temperature is consistent with the observed augmentation in water penetration into the bilayer with increasing temperature (Bernsdorff et al., 1997). The large isothermal variation in  $\tau_c$  with phospholipid acyl chain composition agrees well with recent measurements that showed that water penetration into the bilayer increases markedly with increased acyl chain unsaturation (Huster et al., 1997). The increases in  $\tau_c$  with cholesterol shown in Fig. 1 A are similar to those previously reported for DPH (Straume and Litman, 1987b) and with laurdan fluorescence measurements showing that cholesterol reduces penetration of water into the membrane (Parasassi et al., 1994). Finally, the approximately 3-ns range of values of  $\tau_c$  shown in Table 1 is too great to be accounted for by changes in bilayer index of refraction or orientational order of the probe molecule (Mitchell and Litman, 1998).

The widths of the Lorentzian lifetime distributions  $w$  also depended upon temperature and composition, but the effect of 30 mol % cholesterol varied considerably with acyl chain composition. An increase in the width of the lifetime distribution is indicative of increased heterogeneity of the bilayer environment of the probe molecule (Bernsdorff et al., 1997). This effect is reflected in the increase in  $w$  with increasing temperature observed for most of the acyl chain compositions. In the two dipolyunsaturated PCs, the value of  $w$  was much higher than in all of the other compositions. Below 40°C,  $w$  was generally less than 0.2 ns in all cholesterol-containing phospholipids except in di-22:6 PC and di-20:4 PC, where it was greater than 0.8 ns. The values of  $w$  in Table 1 indicate that DPH in the two dipolyunsaturated species at 10°C experiences a greater degree of environmental heterogeneity than DPH in any of the other species at 40°C. Cholesterol had its smallest effect on  $w$  in the two dipolyunsaturated species. The values of  $w$  in di-18:1 PC, 16:0, 22:6 PC, 16:0, 18:1 PC, and di-14:0 PC were reduced by 30 mol % cholesterol at 30°C by a factor of 5–10, whereas in di-22:6 PC and di-20:4 PC  $w$  was reduced by only a factor of 0.2–0.5, as shown in Fig. 1 B.

The combination of an acyl-chain-dependent effect of cholesterol on  $w$  and an acyl-chain-independent effect of cholesterol on  $\tau_c$  indicates that cholesterol alters the interfacial and hydrophobic core regions of the bilayer via two distinct mechanisms. In the bilayer interfacial region, cholesterol likely forms a hydrogen bond with the carbonyl oxygen (Huang, 1977a,b). The observation that cholesterol raises  $\tau_c$  by providing a barrier to water penetration, in a manner which does not depend on acyl chain composition, implies cholesterol's interaction with PC in the interfacial region is unaffected by changes in acyl chain unsaturation. On the other hand, the acyl-chain-dependent effects of cholesterol on  $w$  suggest that cholesterol changes acyl chain packing in a manner that depends upon acyl chain unsaturation. The small effect of cholesterol on  $w$  in the two dipolyunsaturated PCs indicates that cholesterol is unable to substantially reduce acyl chain packing heterogeneity in

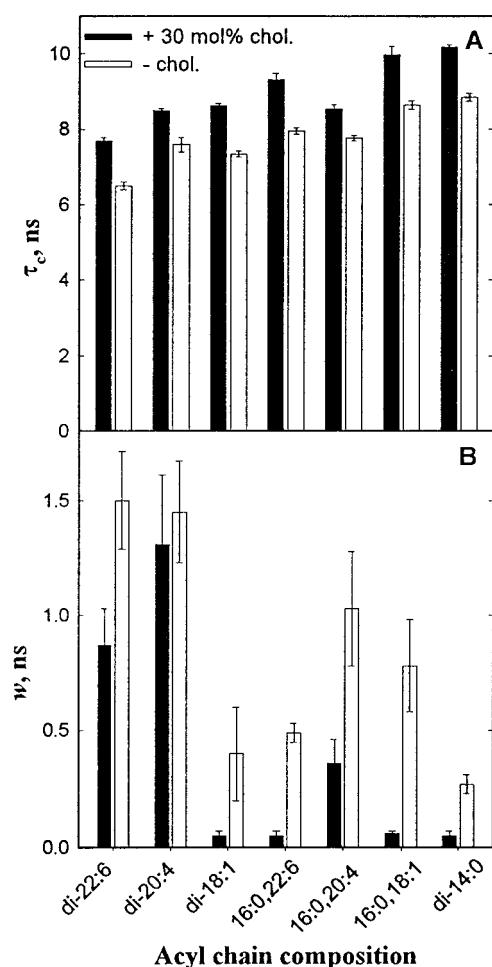


FIGURE 1 Effect of 30 mol % cholesterol on Lorentzian fluorescence lifetime distributions of DPH at 30°C. ((A) Distribution centers  $\tau_c$  for each composition. (B) Distribution widths  $w$  for each composition.



bilayers composed of PCs where both acyl chains have double bonds at positions closer to the carbonyl group than C9. These results are consistent with the findings that van der Waals interactions between acyl chains and cholesterol are primarily responsible for cholesterol's condensing effect on phospholipid bilayers (Cadenhead and Muller-Landau, 1979). Double bonds closer to the carbonyl than C9 would reduce the possible number of favorable van der Waals contacts with the flat  $\alpha$ -face of cholesterol, which is the principal interaction between cholesterol and the acyl chains of PCs (Yeagle et al., 1977).

### Differential polarization

The differential polarization data at all four temperatures was globally analyzed for each phospholipid composition with the BRD model, and the results are summarized in Table 2. A number of studies involving DPH in bilayers (Lentz, 1993) and hydrocarbons (Best et al., 1987) have shown that the value of the initial anisotropy  $r_o$  for DPH depends upon its environment. In our analysis, the initial anisotropy  $r_o$  was globally linked for all temperatures for each bilayer composition, based on the assumption that  $r_o$  varies with bilayer composition but not temperature (Wang et al., 1991). With the exception of di-20:4 PC, the values of  $r_o$  in Table 2 are fairly independent of acyl chain composition and vary from 0.334 to 0.361, which is within the range of values reported in other studies involving significant

variation in bilayer composition (Wang et al., 1991; Velez et al., 1995; Muller et al., 1996). In di-20:4 PC and 16:0, 18:1 PC, 30 mol % cholesterol lowered  $r_o$  by 5.2% and 6.8%, respectively, but in all other bilayers  $r_o$  for the cholesterol-containing bilayers was within 0.8% of the value in a pure phospholipid bilayer (values taken from Mitchell and Litman, 1998). The similar values of  $r_o$  for DPH with and without cholesterol imply that  $r_o$  reflects a property of the hydrophobic bilayer core determined by the phospholipid acyl chain composition.

The wide variation in the order parameters  $\langle P2 \rangle$  and  $\langle P4 \rangle$  with changes in phospholipid acyl chain composition is shown in Fig. 2. The four points for each acyl chain composition in Fig. 2 result from variation in temperature, with the point closest to the origin corresponding to the highest temperature. The progression within each symbol type from lower left to upper right in Fig. 2 demonstrates that decreasing the temperature increases equilibrium order of DPH in a similar manner in bilayers composed of all seven phospholipids plus 30 mol % cholesterol. The groups of symbols also progressively change from lower left to upper right with decreasing unsaturation, showing that increased acyl chain unsaturation results in decreased equilibrium molecular order. The clearest indicators of this trend are the symbols for di-22:6 PC and di-20:4 PC in the lower left and the symbols for di-14:0 PC in the upper right. The dotted line in Fig. 2 shows the relationship between  $\langle P2 \rangle$  and  $\langle P4 \rangle$  corresponding to the wobble-in-cone model (Kinosita et al.,

**TABLE 2** Results of global analysis of differential polarization data with the BRD model

Lipid	$r_o$	°C	$\langle P2 \rangle$		$\langle P4 \rangle$		$D_{\perp}$ (ns <sup>-1</sup> )	
di-22:6 PC	0.357 ± 0.009	10	0.372 ± 0.01		0.377 ± 0.023		0.168 ± 0.018	
		20	0.337	0.010	0.359	0.019	0.240	0.024
		30	0.315	0.009	0.346	0.022	0.371	0.036
		40	0.214	0.010	0.294	0.021	0.623	0.051
di-20:4 PC	0.290 ± 0.004	10	0.505 ± 0.015		0.397 ± 0.021		0.076 ± 0.005	
		20	0.471	0.009	0.365	0.018	0.162	0.010
		30	0.418	0.008	0.325	0.017	0.197	0.010
		40	0.380	0.008	0.293	0.029	0.354	0.019
di-18:1 PC	0.353 ± 0.004	10	0.585 ± 0.010		0.562 ± 0.009		0.053 ± 0.005	
		20	0.536	0.007	0.502	0.009	0.084	0.007
		30	0.514	0.005	0.475	0.008	0.137	0.010
		40	0.474	0.004	0.446	0.009	0.213	0.014
16:0, 22:6 PC	0.334 ± 0.004	10	0.715 ± 0.006		0.561 ± 0.010		0.073 ± 0.05	
		20	0.631	0.005	0.529	0.009	0.167	0.013
		30	0.570	0.007	0.460	0.016	0.207	0.013
		40	0.521	0.004	0.398	0.011	0.281	0.014
16:0, 20:4 PC	0.361 ± 0.004	10	0.610 ± 0.011		0.521 ± 0.013		0.076 ± 0.006	
		20	0.560	0.009	0.503	0.011	0.134	0.011
		30	0.498	0.006	0.461	0.010	0.197	0.014
		40	0.444	0.006	0.427	0.009	0.281	0.018
16:0, 18:1 PC	0.331 ± 0.004	10	0.821 ± 0.008		0.690 ± 0.010		0.029 ± 0.004	
		20	0.738	0.005	0.606	0.009	0.071	0.008
		30	0.674	0.005	0.576	0.010	0.120	0.013
		40	0.592	0.004	0.478	0.011	0.184	0.013
di-14:0 PC	0.342 ± 0.001	30	0.955 ± 0.009		0.902 ± 0.006		0.009 ± 0.002	
		40	0.941	0.004	0.879	0.005	0.033	0.007
		47	0.934	0.003	0.868	0.004	0.061	0.011
		55	0.916	0.003	0.845	0.016	0.167	0.059

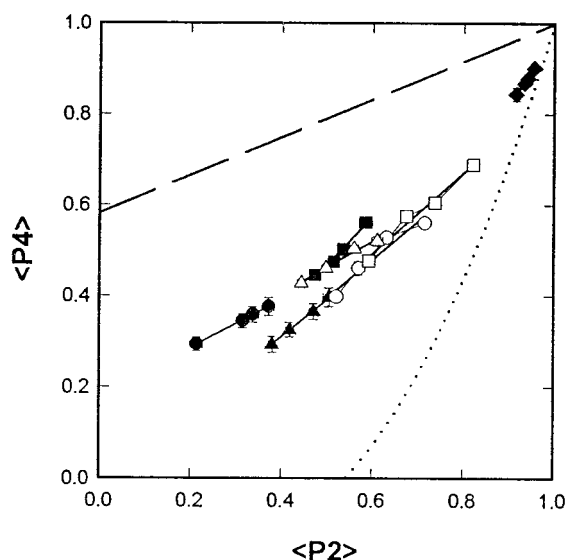


FIGURE 2 Plot of the order parameters  $\langle P_2 \rangle$  versus  $\langle P_4 \rangle$  obtained from the BRD model for DPH in bilayers containing 30 mol % cholesterol and di-22:6 PC (●), di-20:4 PC (▲), di-18:1 PC (■), 16:0, 22:6 PC (○), 16:0, 20:4 PC (△), 16:0, 18:1 PC (□), and di-14:0 PC (◆). Also shown is the relationship between  $\langle P_2 \rangle$  and  $\langle P_4 \rangle$  corresponding to the wobble-in-cone model (···) and the maximal possible values of  $\langle P_4 \rangle$  (---).

1977). This curve is included to show that the wobble-in-cone model was unable to accurately represent the differential polarization data for any acyl chain composition except di-14:0 PC. The dashed line in Fig. 2 corresponds to the maximal value of  $\langle P_4 \rangle$  as a function of  $\langle P_2 \rangle$  (Pottel et al., 1986) and shows that although the values of  $\langle P_4 \rangle$  for di-14:0 PC are quite high they are not above the theoretical maximal values.

Variation in both temperature and acyl chain composition caused a wide range of DPH rotational diffusion coefficients  $D_{\perp}$  (Fig. 3 A). Examination of the data at 30°C and 40°C shows that the biggest differences due to acyl chain composition are between di-22:6 PC and di-14:0 PC. DPH rotational motion in di-22:6 PC/cholesterol is so rapid relative to the motion in other acyl chain compositions that  $D_{\perp}$  in di-22:6 PC/cholesterol at 10°C is equivalent to that observed in di-18:1 PC/cholesterol or 16:0, 18:1 PC/cholesterol at 40°C. The average effect of 30 mol % cholesterol at 30°C and 40°C was to slow the rotational motion of DPH in all acyl chain compositions, except in di-22:6 PC (Fig. 3 B). The reduction in  $D_{\perp}$  due to cholesterol was most pronounced in di-14:0 PC where it was reduced by 92%, whereas in di-22:6 PC it was slightly increased. In the phospholipids with levels of unsaturation between these two extremes,  $D_{\perp}$  was reduced by 5–25%.

The solution to the BRD model given in Table 1 is the high- $\langle P_4 \rangle$  solution and produces bimodal orientational distribution functions,  $f(\theta)$ , with maxima at 0° and 90° (Pottel et al., 1986; Mitchell and Litman, 1998). Extensive examination of the global error surface for each phospholipid composition revealed a second solution to the BRD model for all phospholipids except di-14:0 PC. This second solu-

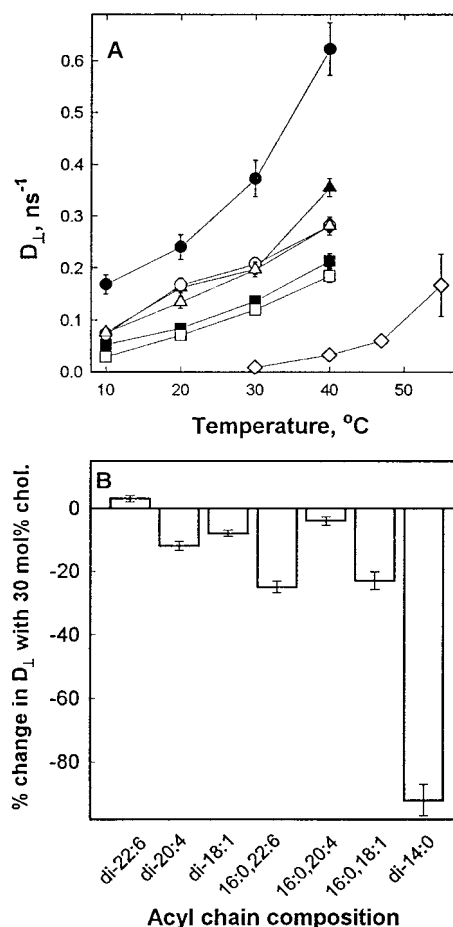


FIGURE 3 Effect of temperature and 30 mol % cholesterol on DPH rotational dynamics. (A)  $D_{\perp}$  as a function of temperature for bilayers containing 30 mol % cholesterol and di-22:6 PC (●), di-20:4 PC (▲), di-18:1 PC (■), 16:0, 22:6 PC (○), 16:0, 20:4 PC (△), 16:0, 18:1 PC (□), and di-14:0 PC (◆). (B) Average decrease in  $D_{\perp}$  induced by 30 mol % cholesterol for 30°C and 40°C.

tion is the low- $\langle P_4 \rangle$  solution, and it produces broad, unimodal orientational distributions with a maximum between 0° and 45° (Mitchell and Litman, 1998). Several previous studies have found instances where these two solutions to the BRD model for DPH in phospholipid bilayers are statistically equivalent (van Langen et al., 1987, 1989; van Ginkel et al., 1989; Wang et al., 1991; Mitchell and Litman, 1998). However, for the cholesterol-containing bilayers examined in this study, the two solutions to the BRD model were not statistically equivalent. The values of  $\chi^2$  for the low- $\langle P_4 \rangle$  solution were 1.5–3 times greater than those for the high- $\langle P_4 \rangle$  solution, and  $F$  tests of the significance of the differences in  $\chi^2$  for the two solutions showed that the high- $\langle P_4 \rangle$  solution was statistically more probable ( $p < 0.01$ ) than the low- $\langle P_4 \rangle$  solution. Thus, only the high- $\langle P_4 \rangle$  solution will be considered in the discussion of the orientational distribution of DPH in these cholesterol-containing bilayers. The bimodal orientational distribution function  $f(\theta)$ , which results from the high- $\langle P_4 \rangle$  solution, corresponds to two orientational populations of DPH in the bilayer. One

population is oriented about the bilayer normal, whereas the second population is oriented about an axis  $90^\circ$  to the bilayer normal, presumably in the bilayer midplane between the two monolayer leaflets. Changes in the fractional size and width of the midplane population provide information about acyl chain ensemble order in the bilayer midplane, whereas changes in the population oriented about the bilayer normal provide information about ensemble acyl chain packing in the region adjacent to the interfacial region (Mitchell and Litman, 1998). The result is an analysis of acyl chain packing throughout the depth of the bilayer that complements the intrachain molecular order profiles obtained from deuterium NMR.

A complete picture of the manner in which the packing of the acyl chains constrains the orientation of DPH in the hydrophobic core of the bilayer is given by the orientational probability distribution  $f(\theta)\sin\theta$ . The orientational probability distribution for DPH in di-14:0 PC with and without 30 mol % cholesterol reveals in detail how the strongly ordering effects of cholesterol on saturated acyl chains reduce the orientational freedom of DPH (Fig. 4 A). In di-14:0 PC/30 mol % cholesterol at  $40^\circ\text{C}$ , more than 95% of the DPH molecules are oriented within  $\sim 20^\circ$  of the bilayer normal, whereas in pure di-14:0 PC at  $40^\circ\text{C}$ , DPH is found in a markedly bimodal distribution with  $\sim 40\%$  of the molecules oriented at angles greater than  $45^\circ$  from the bilayer normal (Fig. 4 A). The population at angles greater than  $45^\circ$  is assumed to consist of DPH in the bilayer midplane, between the two phospholipid monolayers (Mitchell and Litman, 1998). The difference between the two probability distributions (Fig. 4 B) shows in detail the angular orientations from which DPH is excluded by cholesterol in di-14:0 bilayers. The region below the zero line in Fig. 4 B reveals that cholesterol limits all orientations of DPH that are more than  $15^\circ$  away from the bilayer normal, whereas the region above the zero line shows the DPH orientations enhanced by the presence of cholesterol. The very narrow orientational probability distribution for DPH in di-14:0 PC/30 mol % cholesterol demonstrates that cholesterol greatly increases the ensemble order of saturated acyl chains. This increase in ensemble order, demonstrated by the DPH orientational probability distribution, is analogous to the well documented ability of cholesterol to increase the intrachain order of saturated phospholipid acyl chains in the LC phase as determined by NMR measurements (Sankaram and Thompson, 1990; Vist and Davis, 1990).

The effects of phospholipid acyl chain unsaturation on the ability of cholesterol to restrict acyl chain ensemble packing may be seen by comparing the probability distributions in Fig. 4 A with those in Fig. 5. The probability distribution in Fig. 5 that most resembles that of di-14:0/30 mol % cholesterol is the one for 16:0, 18:1 PC/30 mol % cholesterol (Fig. 5 A, dotted curve). This similarity in the effect of cholesterol on di-14:0 PC and 16:0, 18:1 PC is consistent with a study by Tinoco and co-workers that found that cholesterol condensed monolayers consisting of saturated and monounsaturated acyl chains via direct interaction

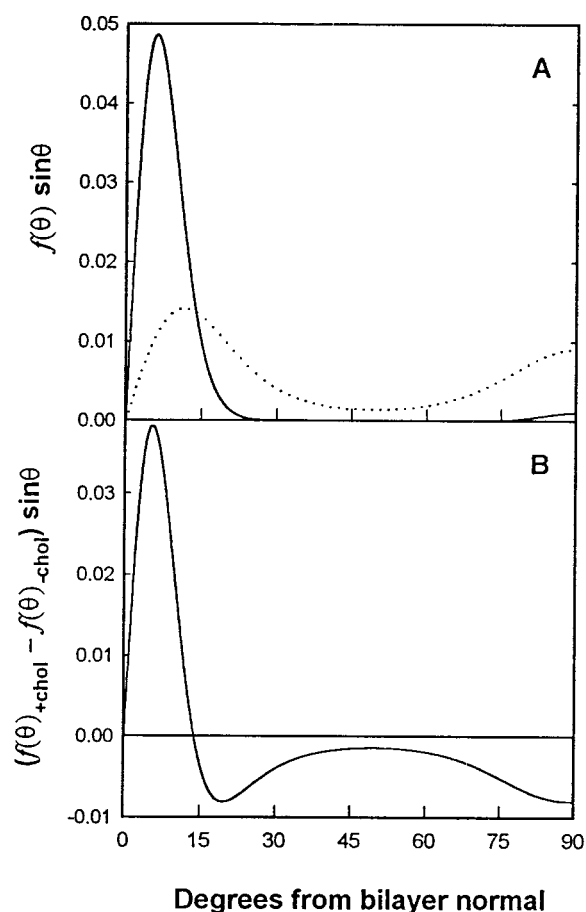


FIGURE 4 Effect of 30 mol % cholesterol on the orientational probability distribution for DPH in di-14:0 PC at  $40^\circ\text{C}$ . (A) The orientational probability distribution for DPH in pure di-14:0 PC ( $\cdots$ ) and di-14:0 PC plus 30 mol % cholesterol (—). (B) Change in the orientational probability distribution due to 30 mol % cholesterol; dotted curve in A subtracted from the solid curve in A.

with the acyl chains (Evans et al., 1987). The probability distribution for DPH in pure di-14:0 PC (Fig. 4 A), is very similar to those for di-22:6 PC/30 mol % cholesterol and di-20:4 PC/30 mol % cholesterol (Fig. 5 B) demonstrating that a dipolyunsaturated bilayer with 30 mol % cholesterol is about as ordered in the bilayer midplane as a cholesterol-free, saturated bilayer at  $40^\circ\text{C}$ .

Direct assessment of the detailed changes in DPH orientational freedom induced by cholesterol is facilitated by examining the difference between the orientational probability distributions obtained with and without cholesterol:  $(f(\theta)_{+\text{chol}} - f(\theta)_{-\text{chol}})\sin\theta$ . The resulting probability difference curves for the phospholipids with an *sn-1* saturated acyl chain in Fig. 6 A show that the effect of cholesterol on the orientation of DPH is gradually reduced with increased unsaturation of the *sn-2* acyl chain. In 16:0, 18:1 PC (dotted line) and 16:0, 20:4 PC (dashed line), 30 mol % cholesterol limits DPH orientations greater than  $30^\circ$  away from the bilayer normal, whereas in 16:0, 22:6 PC (solid line), orientations up to about  $45^\circ$  are allowed. The probability

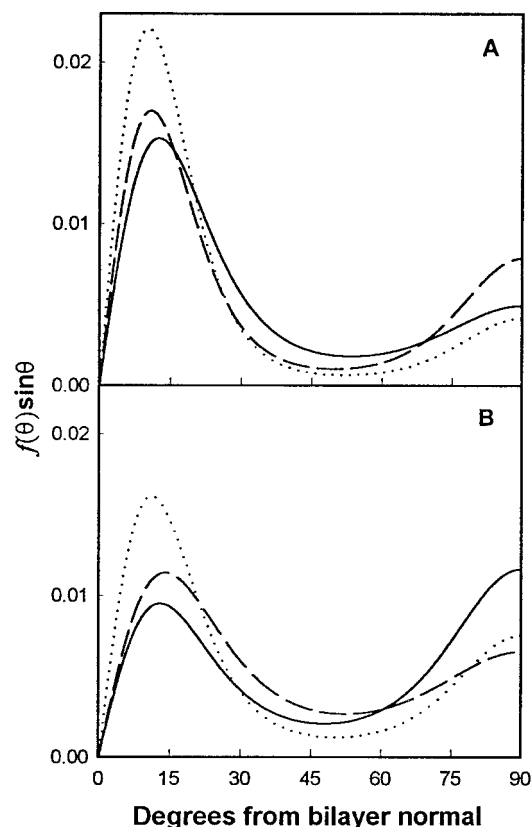


FIGURE 5 Orientational probability distributions for all unsaturated PCs with 30 mol % cholesterol at 40°C. (A) 16:0, 22:6 PC (—), 16:0, 20:4 PC (---), 16:0, and 18:1 PC (···). (B) di-22:6 PC (—), di-20:4 PC (---), and di-18:1 PC (···).

difference curves for the diunsaturated phospholipids in Fig. 6 B show that the effect of 30 mol % cholesterol in these bilayers also varies with acyl chain unsaturation, and the effect is generally less pronounced than that observed in the *sn-1* saturated species. One difference between the symmetric and asymmetric species is the somewhat similar effect of 30 mol % cholesterol on the orientation of DPH in di-18:1 PC (dotted line) and di-20:4 PC (dashed line). The differences in these two curves below the zero line reflect the different orientational probability distributions for DPH in the two cholesterol-free bilayers, but their similarity above the zero line shows that 30 mol % cholesterol transfers orientational probability for DPH into the same angular range in both phospholipids. The profile for di-18:1 PC in Fig. 6 B demonstrates a reduction in bilayer free volume in the bilayer midplane as a result of the interaction of cholesterol with 18:1n9 acyl chains, in contrast to some previous reports (Subczynski et al., 1990; Pasenkiewicz-Gierula et al., 1991). The second difference regarding the symmetric, unsaturated species is the very small effect of 30 mol % cholesterol in di-22:6 PC (solid line). In contrast with the graded effect of cholesterol with acyl chain unsaturation for the *sn-1* saturated phospholipids, in the symmetrically unsaturated phospholipids, the effect of increased unsaturation on the distribution profiles appears to be discontinuous.

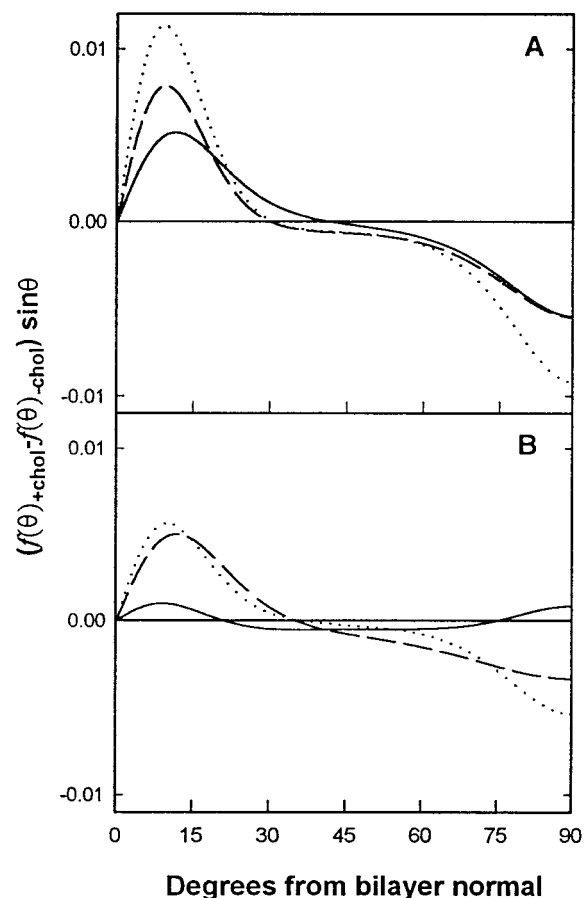


FIGURE 6 Change in the orientational probability distribution due to 30 mol % cholesterol for all unsaturated PCs at 40°C. (A) 16:0, 22:6 PC (—), 16:0, 20:4 PC (---), and 16:0, 18:1 PC (···). (B) di-22:6 PC (—), di-20:4 PC (---), and di-18:1 PC (···).

The cholesterol-induced changes in  $f(\theta)\sin\theta$  in Figs. 4 B and 6 show that cholesterol generally reduces the population of DPH molecules that are oriented at angles greater than 45° from the bilayer normal. The portion of the orientational probability distribution with a maximum at 90° is interpreted as corresponding to a population of DPH molecules located in the bilayer midplane region (Straume and Litman, 1987a; Mitchell and Litman, 1998). The relative size of this population was assessed by calculating  $f_{\perp}$  according to Eq. 3. Variation in the cholesterol-induced changes in  $f_{\perp}$  with acyl chain unsaturation shows how acyl chain unsaturation modulates the extent to which cholesterol alters acyl chain packing near the bilayer midplane (Fig. 7). In all acyl chain compositions  $f_{\perp}$  increased with increasing temperature, although in di-14:0 PC the increase was quite small, as shown in Fig. 7 A. This is consistent with deuterium NMR measurements of acyl chain order as a function of temperature, which show that most of the effect of increased temperature is a decrease in order in the most terminal 8–10 carbons (Lefleur et al., 1989). Acyl chain unsaturation increased  $f_{\perp}$ , and the large difference between di-14:0 PC and 16:0, 18:1 PC shows that the introduction of a 9-*cis* double bond in the



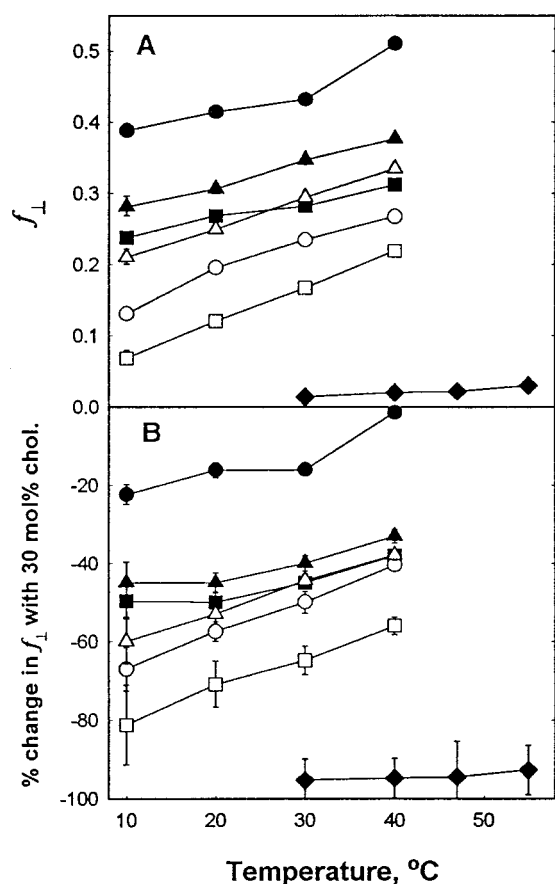


FIGURE 7 Effect of temperature and 30 mol % cholesterol on  $f_{\perp}$ , the fraction of DPH molecules within  $45^{\circ}$  of the plane of the bilayer. (A)  $f_{\perp}$  as a function of temperature in bilayers containing 30 mol % cholesterol. (B) Percentage decrease in  $f_{\perp}$  due to 30 mol % cholesterol for di-22:6 PC (●), di-20:4 PC (▲), di-18:1 PC (■), 16:0, 22:6 PC (○), 16:0, 20:4 PC (△), 16:0, 18:1 PC (□), and di-14:0 PC (◆).

*sn*-2 chain sharply diminishes cholesterol's ability to exclude DPH from the bilayer midplane. A second notable increase in  $f_{\perp}$  is found at the other end of the unsaturation spectrum where  $f_{\perp}$  increases 0.36–0.52 upon going from di-20:4 PC to di-22:6 PC. This large increase in  $f_{\perp}$  demonstrates that di-22:6 PC is uniquely able to limit the ordering effect of cholesterol in the bilayer midplane.

Acyl chain composition had a marked effect on the ability of 30 mol % cholesterol to increase acyl chain packing order in the bilayer midplane region and thereby exclude DPH from the bilayer midplane. The most striking example of this compositional dependence is the fact that cholesterol has a greater ability to order the midplane region of bilayer with exclusively 20:4 acyl chains than a bilayer with exclusively 22:6 acyl chains. This is apparent from the large difference between  $f_{\perp}$  with and without cholesterol for di-22:6 PC (filled circles) and di-20:4 PC (filled triangles) in Fig. 7 B. The difference in the effect of cholesterol between these two dipolyunsaturated phospholipids suggests that polyunsaturated n3 acyl chains interact much more weakly with cholesterol than do polyunsaturated n6

acyl chains. Apparently, this difference is of secondary importance for phospholipids with an *sn*-1 saturated acyl chain, as the effects of cholesterol on  $f_{\perp}$  in 16:0, 20:4 PC (open triangles) and in 16:0, 22:6 PC (open circles) are essentially identical (Fig. 7 B).

The size of the fractional population of DPH oriented about the bilayer midplane is not correlated with the width of Lorentzian lifetime distribution  $w$ . Both di-22:6 PC/cholesterol and di-20:4 PC/cholesterol have very large values of  $w$ , as shown in Table 1, and they have the largest values of  $f_{\perp}$ , as shown in Fig. 7 A. However,  $w$  decreases dramatically in the more saturated PCs, whereas only an incremental decrease in  $f_{\perp}$  with increasing saturation is observed. In addition,  $f_{\perp}$  exhibits a clear upward trend with increasing temperature from 10°C to 40°C, whereas  $w$  is basically unchanged below 40°C in all bilayer compositions.

Acyl-chain-dependent alteration of  $f_{\perp}$  by cholesterol is informative with respect to the ability of cholesterol to increase ensemble order in the bilayer midplane, but the ordering effects of cholesterol throughout the bilayer are best assessed by considering the extent to which cholesterol prevents DPH from adopting a random orientational distribution. This is equivalent to assessing the extent to which  $f(\theta)\sin\theta$  differs from a random orientational distribution without special consideration given to any particular range of orientations. This type of comparison is easily accomplished via the free volume parameter  $f_v$  (Straume and Litman, 1987a), given in Eq. 4. This parameter has been shown to be directly proportional to the overlap between  $f(\theta)\sin\theta$  and a random orientational distribution (Mitchell and Litman, 1998). Both increased temperature and acyl chain unsaturation raise the value of  $f_v$ , in agreement with previous measurements on several of these cholesterol-containing bilayers (Straume and Litman, 1987b).

The three groupings in Fig. 8 A provide a succinct summary of the properties of the set of cholesterol-containing bilayers examined in this study. The lowest values of  $f_v$  were obtained for di-14:0 PC, demonstrating that a bilayer consisting of disaturated acyl chains and cholesterol severely limits the orientational freedom of a cylindrical probe molecule like DPH. The group of cholesterol-containing bilayers that afford an intermediate amount of orientational freedom for DPH are those with an *sn*-1 saturated acyl chain and di-18:1 PC. The importance of unsaturation of the *sn*-2 chain is shown by the relative values of  $f_v$  at 40°C for the series 16:0, 22:6 PC, 16:0, 20:4 PC, 16:0, 18:1 PC, in accord with previous measurements (Straume and Litman, 1987b). The grouping of di-18:1 PC with the *sn*-1 saturated species is in agreement with a recent monolayer study that found that the elastic area compressibility modulus of di-18:1 PC/cholesterol was lower than that of 16:0, 18:1 PC/cholesterol but greater than that of 16:0, 20:4 PC/cholesterol or 16:0, 22:6 PC/cholesterol (Smaby et al., 1997). The greatest degree of orientational freedom was obtained in the two dipolyunsaturated PC/cholesterol bilayers, the  $f_v$  values of which at 10°C are higher than the  $f_v$  values in all other bilayers at 40°C. The large values of  $f_v$  obtained in the two

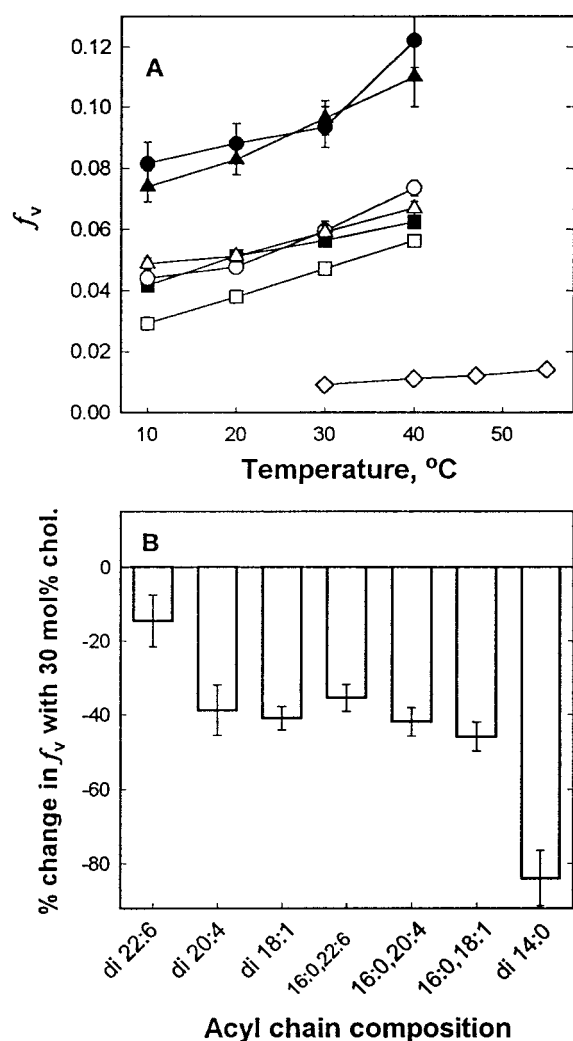


FIGURE 8 Effect of temperature and 30 mol % cholesterol on  $f_v$ , the fractional free volume parameter (defined in Eq. 5). (A)  $f_v$  as a function of temperature in bilayers containing 30 mol % cholesterol and di-22:6 PC (●), di-20:4 PC (▲), di-18:1 PC (■), 16:0, 22:6 PC (○), 16:0, 20:4 PC (△), 16:0, 18:1 PC (□), or di-14:0 PC (◆). (B) Decrease in  $f_v$  induced by 30 mol % cholesterol, averaged over all four temperatures.

dipolyunsaturated/cholesterol bilayers demonstrate that the relatively loose packing of polyunsaturated acyl chains is maintained even in the presence of 30 mol % cholesterol.

The extent to which  $f_v$  was altered by cholesterol (Fig. 8 B) quantifies the changes in  $f(\theta)\sin\theta$  is shown in Fig. 6 and further demonstrates the singularly weak interaction of 22:6 acyl chains with cholesterol. When both acyl chains are 22:6, the presence of 30 mol % cholesterol reduces  $f_v$  by less than one-half the amount observed in all other acyl chain compositions examined. At the other end of the spectrum, the almost complete loss of free volume caused by adding 30 mol % cholesterol to di-14:0 PC demonstrates the pronounced ability of cholesterol to order saturated acyl chains. The very low values of  $f_v$  for di-14:0 PC plus 30 mol % cholesterol are a quantitative measure of the very narrow, unimodal orientational distribution function shown

in Fig. 4 A. The surprising aspect of Fig. 8 B is that it shows that cholesterol reduces  $f_v$  on a percentage basis approximately equally in the three *sn-1* saturated, *sn-2* unsaturated PCs as well as di-18:1 PC and di-20:4 PC. Fig. 8 A shows that the actual value of  $f_v$  in each of these five different cholesterol-containing bilayers is strictly correlated with the extent of acyl chain unsaturation; however, their similar percentage reduction in  $f_v$  underlines the unique nature of di-22:6 PC to resist the ordering effect of cholesterol. The decrease in  $f_v$  for di-20:4 PC shown in Fig. 8 B shows that cholesterol is able to modify the packing of 20:4 acyl chains. However, the actual values of  $f_v$  for di-20:4 PC/cholesterol in Fig. 8 A demonstrate that the di-20:4 PC/cholesterol bilayer provides DPH approximately as much orientational freedom as the di-22:6 PC/cholesterol bilayer. The large difference in the effect of cholesterol between 16:0, 18:1 PC and di-14:0 PC shows that both chains must be saturated for the strength of the cholesterol-saturated chain interaction to manifest itself completely. Similarly, the difference in the effect of cholesterol between 16:0, 22:6 PC and di-22:6 PC shows that both chains must be 22:6 before the weakness of the cholesterol-22:6 chain interaction can take full effect. The contrast between the large cholesterol-induced changes reported by DPH in 16:0, 22:6 PC and the minimal changes observed in di-22:6 PC demonstrates that DPH partitions into bilayer regions that are rich in cholesterol and saturated acyl chains and is sensitive to changes in acyl chain packing in these regions.

The suggestion that the cholesterol-20:4n6 interaction is stronger than the cholesterol-22:6n3 interaction (Fig. 8 B) would appear to contradict a study showing that cholesterol condenses monolayers and bilayers composed of 18:0, 18:3n3 PC but not those composed of 18:0, 18:3n6 PC (Stillwell et al., 1994). However, the present study supports the primary conclusion of Stillwell et al. (1994) and others (Huang, 1977a,b) that cholesterol interacts most strongly with acyl chains that do not have a double bond closer to the carbonyl than C9-C10. In the present study, only di-20:4 PC and di-22:6 PC did not have at least one acyl chain with a double bond beyond the C9. In these two PCs, with 30 mol % cholesterol, DPH had the greatest level of rotational and orientational freedom.

The distinction that the present study draws between 20:4n6 and 22:6n3 has to do with the methyl ends of these molecules where 20:4n6 has five saturated carbons and 22:6n3 has only two. This means that in a 20:4n6 bilayer the bilayer midplane consists of a zone ~10 carbon-carbon bonds thick where there are no double bonds, whereas in a 22:6n3 bilayer this zone is only ~4 carbon-carbon bonds thick. The analysis employed in this study is particularly sensitive to changes in acyl chain packing in the bilayer midplane region, and it is in this region that the major differences between di-20:4 PC/cholesterol and di-22:6/cholesterol are detected, as shown in Figs. 6 B and 7 B. Sensitivity to packing in the bilayer midplane probably accounts for our detection of a difference between the effect of cholesterol on acyl chain packing in di-22:6 and di-20:4,

whereas a recent monolayer study found that cholesterol had essentially no effect on the elastic area compressibility modulus of both di-22:6 PC and di-20:4 PC monolayers (Smaby et al., 1997).

## CONCLUSIONS

Analysis of DPH anisotropy decay data in terms of the BRD model leads to the angular orientational probability distribution of DPH,  $f(\theta)\sin\theta$ , which reflects phospholipid acyl chain ensemble order throughout the depth of the bilayer, as shown in Figs. 4 *A* and 5. Examination of the changes in  $f(\theta)\sin\theta$  induced by cholesterol illustrates in detail how cholesterol-induced changes in acyl chain ensemble order depend upon acyl chain composition, as shown in Figs. 4 *B* and 6. Two significant conclusions regarding cholesterol and polyunsaturated acyl chains may be drawn from the results presented in this study. The first concerns whether there is an acyl chain composition capable of producing a cholesterol-containing bilayer with relatively loose acyl chain packing and a high degree of lateral compressibility. Among the phospholipids examined in this study, only the di-20:4 PC/cholesterol and di-22:6 PC/cholesterol bilayers afforded DPH a high level of orientational freedom (Fig. 8 *A*) and a highly heterogeneous environment (Fig. 1 *B*). This conclusion regarding the effect of cholesterol in di-20:4 PC and di-22:6 PC is supported by measurements of the effect of cholesterol on lateral compressibility in di-20:4 PC bilayers (Needham and Nunn, 1990) and di-20:4 PC and di-22:6 PC monolayers (Smaby et al., 1997).

The second conclusion concerns the role of acyl chain unsaturation in determining the strength of cholesterol-acyl chain interactions. The results summarized in Figs. 6 *B*, 7 *B*, and 8 *B* all indicate that cholesterol alters acyl chain packing in di-22:6 PC to a smaller extent than it does in di-20:4 PC. This is interpreted as indicating that the interaction of cholesterol with 22:6n3 is the weakest of all of the acyl chains examined in this study. Taken together with the strong interaction of cholesterol with saturated chains, this implies that lateral microdomains could form based purely on the relative strength of acyl chain-acyl chain interactions and cholesterol-acyl chain interactions. Such a model was first suggested for mixed-chain, saturated polyunsaturated PCs by vibrational spectroscopy studies (Litman et al., 1991).

A schematic model of cholesterol and unsaturation-driven microdomains in a bilayer consisting of cholesterol, 16:0, 22:6 PC, and di-22:6 is shown in Fig. 9. Fig. 9 *A* depicts a bilayer cross section showing the preferred interaction of cholesterol with the saturated, 16:0 acyl chains. Fig. 9 *B* shows cholesterol and only the acyl chains of the phospholipid in a top view of the bilayer midplane. The segregation of all of the cholesterol and saturated acyl chains into cholesterol-saturated acyl chain microdomains is intended to show what such microdomains might look like on the 10-ns time scale of fluorescence. In a real membrane, such microdomains would be constantly in flux, forming

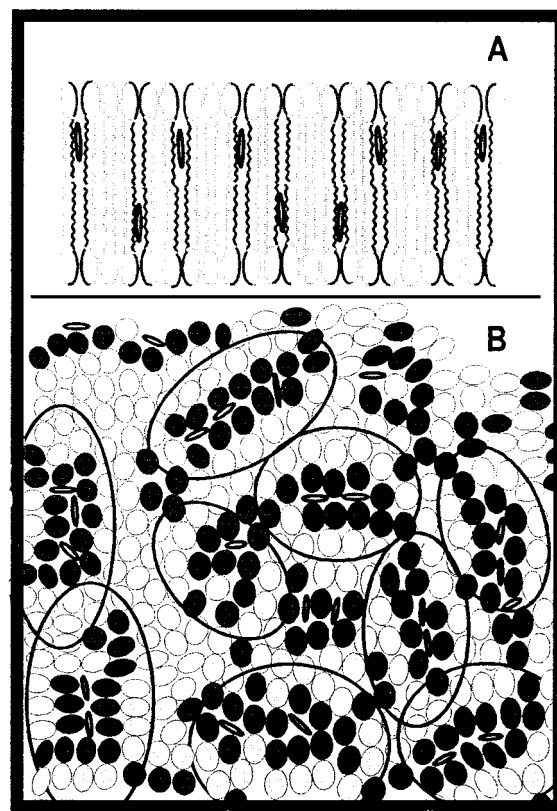


FIGURE 9 Microdomain model for acyl chain packing in a phospholipid bilayer consisting of dipolyunsaturated and mixed chain polyunsaturated phosphatidylcholines and cholesterol. (*A*) Transverse view of the bilayer showing the saturated (black) and polyunsaturated (light gray) phospholipid acyl chain packing. Cholesterol is represented by gray ovals. (*B*) Top view of the bilayer midplane, in which the PC molecules are represented by pairs of circles representing the *sn*-1 chain and *sn*-2 chain. Cholesterol is represented by gray ovals. The large black ovals circumscribe predominantly mixed acyl chain phospholipid domains containing cholesterol. The packing of the mixed chain PCs is with the saturated *sn*-1 chains oriented toward the tightly packed interior of the domain and the polyunsaturated *sn*-2 chains oriented toward the domain boundary. The dipolyunsaturated PCs form the connected phase between microdomains. The domains are highly dynamic structures in the LC phase, and this figure represents a snapshot of the arrangement of the lipids. The domains have a characteristic lifetime and size, which can be influenced by the partitioning of lipid-soluble molecules, such as cholesterol, into the bilayer.

and dispersing rapidly. The strong preferential interaction of cholesterol with saturated chains drives its localization to the interior of the domains. Therefore, cholesterol can reduce the free volume of the bilayer by ordering the saturated *sn*-1 chains in the domain interior, leaving domain-domain interactions unchanged. The connected phase between the microdomains consists of polyunsaturated acyl chains; therefore, it is expected that lateral compressibility will be governed by the polyunsaturated acyl chains. As a result, the lateral compressibility will be relatively unchanged by additional cholesterol added to the bilayer. Direct measurements of lateral compressibility demonstrate that the addition of cholesterol has very little effect on the lateral compressibility of dipolyunsaturated PC bilayers (Needham and



Nunn, 1990) and monolayers (Smaby et al., 1997). A variety of measurements have shown that the interaction between a saturated acyl chain and either 20:4n6 or 22:6n3 is much weaker than the interaction between two saturated acyl chains (Holte et al., 1995; Kariel et al., 1991; Hernandez-Borrell and Keough, 1993). Thus, there will be a tendency to form the type of microdomains in Fig. 9 even in the absence of cholesterol, as has been suggested by vibrational spectroscopy studies (Litman et al., 1991). This model is further supported by differential scanning calorimetry measurements on di-16:0 PC/di-22:6 PC/cholesterol mixtures that show that cholesterol partitions exclusively into the di-16:0 PC phase of these mixed systems (Niebylski and Litman, unpublished results).

The microdomain model shown in Fig. 9 is consistent at a molecular level with all of the results of the many studies performed on model systems made from cholesterol and polyunsaturated phospholipids. In addition, it is consistent with a series of studies carried out in this laboratory that have shown that bilayer cholesterol inhibits the formation of the metarhodopsin II intermediate in photoactivated rhodopsin by decreasing bilayer free volume (Mitchell et al., 1990, 1992; Litman and Mitchell, 1996). These studies demonstrated that the basic relationship between bilayer free volume and rhodopsin conformational equilibrium is unaltered by bilayer cholesterol, implying that although cholesterol reduced bilayer free volume, the lateral compressibility of the bilayer was unchanged. The requisite conditions for the creation of cholesterol-saturated acyl chain microdomains, i.e., the presence of asymmetric and symmetric polyunsaturated phospholipids and cholesterol, are found in many important biological membranes such as the retinal rod outer segment, postsynaptic membranes, and sperm heads (Salem, 1989). For instance, in the retinal rod outer segment, phospholipids with two polyunsaturated acyl chains and with *sn*-1 saturated, *sn*-2 polyunsaturated acyl chains account for 20% and 45%, respectively, of total membrane phospholipid (Stinson et al., 1991). Therefore, there is good reason to believe that application of this microdomain model to biological membranes, the lipid composition of which is similar to the rod outer segment disk, will lead to a greater understanding of the molecular mechanisms involved in modulation of membrane protein function by compositionally determined membrane structure and physical properties.

## REFERENCES

- Alcala, J. R., E. Gratton, and F. G. Prendergast. 1987. Resolvability of lifetime distributions using phase fluorometry. *Biophys. J.* 51:587–596.
- Bartlett, G. R. 1959. *J. Biol. Chem.* 234:466–468.
- Beechem, J. M., E. Gratton, M. Ameloot, J. R. Knutson, and L. Brand. 1991. The global analysis of fluorescence intensity and anisotropy decay data. In *Second Generation Theory and Programs: Topics in Fluorescence Spectroscopy*, Vol. 2, Principles. J. R. Lakowicz, editor. Plenum Press, New York. 241–305.
- Bergelson, L. O., K. Gawrisch, J. A. Ferretti, and R. Blumenthal. 1995. Domain organization in biological membranes. *Mol. Membr. Biol.* 12:1–162.
- Bernsdorff, C., A. Wolf, R. Winter, and E. Gratton. 1997. Effect of hydrostatic pressure on water penetration and rotational dynamics in phospholipid-cholesterol bilayers. *Biophys. J.* 72:1264–1277.
- Best, L., E. John, and F. Jahnig. 1987. Order and fluidity of lipid membranes as determined by fluorescence anisotropy decay. *Eur. Biophys. J.* 15:87–102.
- Cadenhead, D. A., and F. Muller-Landau. 1979. Molecular packing in steroid-lecithin monolayers. III. Mixed films of 3-doxyl cholestane and 3-doxyl-17-hydroxyl-androstane with dipalmitoylphosphatidylcholine. *Chem. Phys. Lipids.* 25:329–343.
- Evans, R. W., M. A. Williams, and J. Tinoco. 1987. Surface areas of 1-palmitoyl phosphatidylcholines and their interactions with cholesterol. *Biochem. J.* 245:455–462.
- Hernandez-Borrell, J., and K. M. W. Keough. 1993. Heteroacid phosphatidylcholines with different amounts of unsaturation respond differently to cholesterol. *Biochim. Biophys. Acta.* 1153:277–282.
- Holte, L. L., S. A. Peter, T. M. Sinnwell, and K. Gawrisch. 1995.  $^2\text{H}$  nuclear magnetic resonance order profiles suggest a change of molecular shape for phosphatidylcholines containing a polyunsaturated acyl chain. *Biophys. J.* 68:2396–2403.
- Huang, C. H. 1977a. Configurations of fatty acyl chains in egg phosphatidylcholine-cholesterol mixed bilayers. *Chem. Phys. Lipids.* 19:150–158.
- Huang, C. H. 1977b. A structural model for the cholesterol-phosphatidylcholine complexes in biological membranes. *Lipids.* 12:348–356.
- Huster, D., A. J. Jin, K. Arnold, and K. Gawrisch. 1997. Water permeability of polyunsaturated lipid membranes measured by  $^{17}\text{O}$  NMR. *Biophys. J.* 73:855–864.
- Johnson, M. L., and L. M. Faunt. 1992. Parameter estimation by least squares methods. *Methods Enzymol.* 210:1–37.
- Kariel, N., E. Davidson, and K. Keough. 1991. Cholesterol does not remove the gel liquid crystalline phase transition of phosphatidylcholines containing two polyenoic acyl chains. *Biochim. Biophys. Acta.* 1062:70–76.
- Kinosita, K., Jr., S. Kawato, and A. Ikegami. 1977. A theory of fluorescence depolarization decay in membranes. *Biophys. J.* 20:289–305.
- Lakowicz, J. R., H. Cherek, and A. Balter. 1981. Correction of timing errors in photomultiplier tubes used in phase modulation fluorometry. *J. Biochem. Biophys. Methods.* 5:131–146.
- Lefleur, M., B. Fine, E. Sternin, P. R. Cullis, and M. Bloom. 1989. Smoothed orientational order profiles of lipid bilayers by  $^2\text{H}$  nuclear magnetic resonance. *Biophys. J.* 56:1037–1041.
- Lentz, B. R. 1993. Use of fluorescence probes to monitor molecular order and motions within liposome bilayers. *Chem. Phys. Lipids.* 64:99–116.
- Levine, Y. K., and G. van Ginkel. 1994. Molecular dynamics in liquid-crystalline systems studied by fluorescence depolarization techniques. In *The Molecular Dynamics of Liquid Crystals*. G. R. Luckhurst and C. A. Veracini, editors. Kluwer Academic, Dordrecht, The Netherlands. 537–571.
- Litman, B. J., E. N. Lewis, and I. W. Levine. 1991. Packing characteristics of highly unsaturated bilayer lipids: Raman spectroscopic studies of multilamellar phosphatidylcholine dispersions. *Biochemistry.* 30:313–319.
- Litman, B. J., and D. C. Mitchell. 1996. A role for phospholipid polyunsaturation in modulating membrane protein function. *Lipids.* 31:s193–s197.
- Mitchell, D. C., and B. J. Litman. 1998. Molecular order and dynamics in bilayers consisting of highly polyunsaturated phospholipids. *Biophys. J.* 74:879–891.
- Mitchell, D. C., M. Straume, and B. J. Litman. 1992. Role of *sn*-1 saturated, *sn*-2 polyunsaturated phospholipids in control of membrane receptor conformational equilibrium: effects of cholesterol and acyl chain unsaturation on the metarhodopsin I:metarhodopsin II equilibrium. *Biochemistry.* 31:662–670.
- Mitchell, D. C., M. Straume, J. L. Miller, and B. J. Litman. 1990. Modulation of metarhodopsin formation by cholesterol-induced ordering of bilayer lipids. *Biochemistry.* 29:9143–9149.
- Muller, J. M., G. van Ginkel, and E. E. van Faassen. 1996. Effect of lipid molecular structure and gramicidin A on the core of lipid vesicle bilayers: a time-resolved fluorescence study. *Biochemistry.* 35:488–497.



- Needham, D., and R. S. Nunn. 1990. Elastic deformation and failure of lipid membranes containing cholesterol. *Biophys. J.* 58:997–1009.
- Parasassi, T., M. Di Stefano, M. Loiero, G. Ravagnan, and E. Gratton. 1994. Cholesterol modifies water concentration and dynamics in phospholipid bilayers: a fluorescence study using laurdan probe. *Biophys. J.* 66:763–768.
- Pasenkiewicz-Gierula, M., W. K. Subczynski, and A. Kusumi. 1990. Rotational diffusion of a steroid molecule in phosphatidylcholine-cholesterol membranes: fluid-phase microimmiscibility in unsaturated phosphatidylcholine-cholesterol membranes. *Biochemistry*. 29: 4059–4069.
- Pasenkiewicz-Gierula, M., W. K. Subczynski, and A. Kusumi. 1991. Influence of phospholipid unsaturation on the cholesterol distribution in membranes. *Biochimie*. 73:1311–1316.
- Pottel, H., W. Herreman, B. W. van Der Meer, and M. Ameloot. 1986. On the significance of the fourth-rank orientational order parameter of fluorophores in membranes. *Chem. Phys.* 102:37–44.
- Salem, N., Jr. 1989. Fatty acids: molecular and biochemical aspects. In *New Protective Roles For Selected Nutrients*. G. A. Spiller and J. Scala, editors. Alan R. Liss, New York. 109–228.
- Sankaram, M. B., and T. E. Thompson. 1990. Modulation of phospholipid acyl chain order by cholesterol. A solid-state  $^2\text{H}$  nuclear magnetic resonance study. *Biochemistry*. 29:10676–10684.
- Schroeder, F., and W. G. Wood. 1995. Lateral lipid domains and membrane function. In *Cell Physiology Source Book*. N. Sperelakis, editor. Academic Press, San Diego. 36–44.
- Smaby, J. M., M. M. Momsen, H. L. Brockman, and R. E. Brown. 1997. Phosphatidylcholine acyl unsaturation modulates the decrease in interfacial elasticity induced by cholesterol. *Biophys. J.* 73:1492–1505.
- Stillwell, W., W. D. Ehringer, A. C. Dumauual, and S. R. Wassall. 1994. Cholesterol condensation of  $\alpha$ -linolenic and  $\gamma$ -linolenic acid-containing phosphatidylcholine monolayers and bilayers. *Biochim. Biophys. Acta*. 1214:131–136.
- Stillwell, W., T. Dallman, A. C. Dumauual, F. T. Crump, and L. J. Jenks. 1996. Cholesterol versus  $\alpha$ -tocopherol: effects on properties of bilayers made from heteroacid phosphatidylcholines. *Biochemistry*. 35: 13353–13362.
- Stinson, A. M., R. D. Wiegand, and R. E. Anderson. 1991. Fatty acid and molecular species compositions of phospholipids and diacylglycerols from rat retinal membranes. *Exp. Eye Res.* 52:213–218.
- Straume, M., and B. J. Litman. 1987a. Equilibrium and dynamic structure of large, unilamellar, unsaturated acyl chain phosphatidylcholine vesicles: higher order analysis of 1,6-diphenyl-1,3,5-hexatriene and 1-[4-(trimethylammonio)phenyl]-6-phenyl-1,3,5-hexatriene anisotropy decay. *Biochemistry*. 26:5113–5120.
- Straume, M., and B. J. Litman. 1987b. Influence of cholesterol on equilibrium and dynamic bilayer structure of unsaturated acyl chain phosphatidylcholine vesicles as determined from higher order analysis of fluorescence anisotropy decay. *Biochemistry*. 26:5121–5126.
- Straume, M., S. G. Frasier-Cadoret, and M. L. Johnson. 1991. Least-squares analysis of fluorescence data. In *Topics in Fluorescence Spectroscopy*, Vol. 2. J. Lakowicz, editor. Plenum Press, New York. 177–240.
- Subczynski, W. K., W. E. Antholine, J. S. Hyde, and A. Kusumi. 1990. Microimmiscibility and three-dimensional dynamic structures of phosphatidylcholine-cholesterol membranes: translational diffusion of a copper complex in the membrane. *Biochemistry*. 29:7936–7945.
- Szabo, A. 1984. Theory of fluorescence depolarization in macromolecules and membranes. *J. Chem. Phys.* 81:150–167.
- van der Meer, B. W., R. P. H. Kooyman, and Y. K. Levine. 1982. A theory of fluorescence depolarization in macroscopically ordered membrane systems. *Chem. Phys.* 66:39–46.
- van der Meer, B. W., H. Pottel, W. Herreman, M. Ameloot, H. Hendrickx, and H. Schroder. 1984. Effect of orientational order on the decay of the fluorescence anisotropy in membrane suspensions. *Biophys. J.* 46: 515–523.
- van Ginkel, G., H. van Langen, and Y. K. Levine. 1989. The membrane fluidity concept revisited by polarized fluorescence spectroscopy on different model membranes containing unsaturated lipids and sterols. *Biochimie*. 71:23–32.
- van Langen, H., Y. K. Levine, M. Ameloot, and H. Pottel. 1987. Ambiguities in the interpretation of time-resolved fluorescence anisotropy measurements on lipid vesicle systems. *Chem. Phys. Lett.* 140:394–400.
- van Langen, H., G. van Ginkel, D. Shaw, and Y. K. Levine. 1989. The fidelity of response of 1-[4-(trimethylammonio)phenyl]-6-phenyl-1,3,5-hexatriene in time-resolved fluorescence anisotropy measurements on lipid vesicles. *Eur. Biophys. J.* 17:37–44.
- Velez, M., M. P. Lillo, A. U. Acuna, and J. Gonzales-Rodriguez. 1995. Cholesterol effect on the physical state of lipid multibilayers from the platelet plasma membrane by time-resolved fluorescence. *Biochim. Biophys. Acta*. 1235:343–350.
- Vist, M. R., and J. D. Davis. 1990. Phase equilibria of cholesterol/dipalmitoylphosphatidylcholine mixtures:  $^2\text{H}$  nuclear magnetic resonance and differential scanning calorimetry. *Biochemistry*. 29:451–464.
- Wang, S., J. M. Beechem, E. Gratton, and M. Glaser. 1991. Orientational distribution of 1,6-diphenyl-1,3,5-hexatriene in phospholipid vesicles as determined by global analysis of frequency domain fluorimetry data. *Biochemistry*. 30:5565–5572.
- Yeagle, P. Y., R. B. Martin, A. K. Lala, H. K. Lin, and K. Bloch. 1977. Differential effects of cholesterol and lanosterol on artificial membranes. *Proc. Natl. Acad. Sci. U.S.A.* 74:4924–4926.
- Zerouga, M., L. J. Jenks, and W. Stillwell. 1995. Comparison of phosphatidylcholines containing one or two docosahexaenoic acyl chains on properties of phospholipid monolayers and bilayers. *Biochim. Biophys. Acta*. 1236:266–272.